TUMOR CELL CLASSIFICATION BASED ON INSTANTANEOUS YOUNG'S MODULUS USING CONSTRICTION CHANNEL BASED MICROFLUIDIC DEVICES

Y. Luo[1], D. Chen[1], Y. Zhao[1], C. Wei[1], X. Zhao[2], W. Yue[2], R. Long[3*], J. Wang[1*] and J. Chen[1*]

[1]*State Key Lab of Transducer Technology, Chinese Academy of Sciences, P.R. China*

[2]*Department of Cellular and Molecular Biology, Capital Medical University, P.R. China*

[3]*Department of Mechanical Engineering, University of Alberta, Canada*

ABSTRACT

This paper presents a microfluidic system enabling continuous characterization of instantaneous Young's modulus ($E_{instantaneous}$) of single cells where cells were aspirated continuously through a constriction channel with cellular entry processes monitored. Both experimental observations and numerical simulations confirmed the two-stage cellular entry process into the constriction channel: an instantaneous jump into the channel ($L_{instantaneous}$) followed by a creeping increase in aspiration length terminated by transitional aspiration length ($L_{transitional}$). Numerical simulations reveal that $L_{instantaneous}$ and $L_{transitional}$ are functions of $E_{instantaneous}$ (linear function) and f_c. By combining measured experimental results with numerical simulations, $E_{instantaneous}$ and f_c were quantified as 3.48±0.86 kPa and 0.39±0.11 for A549 cells (n_{cell}=199), 2.99±0.38 kPa and 0.37±0.02 for 95C cells (n_{cell}=164), 5.24±0.74 kPa and 0.37±0.02 for 95D cells (n_{cell}=143). As a platform technology, this method may function as a new approach for cellular mechanical property characterization.

KEYWORDS: Microfluidic, Cellular Biophysics, Single-Cell Analysis, Instantaneous Young's Modulus, Constriction Channel

INTRODUCTION

Intrinsic cellular mechanical properties (e.g., instantaneous Young's modulus ($E_{instantaneous}$) and equilibrium Young's modulus ($E_{equilibrium}$)) have been regarded as label-free biophysical markers for tumor cell classification.[1] Conventional techniques (e.g., atomic force microscopy) only reported Young's modulus from tens of tumor cells with limited statistical significances.[2] Meanwhile, microfluidics offer continuous tumor cell mechanical property characterization based on constriction channel[3] or hydrodynamic stretching[4]. However, these microfluidic devices can't collect intrinsic cellular mechanical properties (e.g., Young's modulus) due to limitations in modeling issues and thus their applications in tumor cell classification are compromised.

To address these issues, in this study, numerical simulations were used to model the cellular entry process into the constriction channel where a cellular viscoelastic model rather than a liquid droplet model was used. In addition, the cellular friction with the constriction channel walls was properly addressed. By combing experimental results with numerical simulations, cellular instantaneous Young's modulus $E_{instantaneous}$ from hundreds of cells were quantified using the constriction channel based microfluidic platform. This technique has a throughput of several cells per minute, two orders of magnitude improvement compared to conventional techniques with throughputs of several cells per hour.

MATERIALS AND METHODS

Cell Culture

Three lung tumor cell lines of A549, 95C and 95D were cultured with RPMI-1640 media supplemented with 10% fetal bovine serum and 1% penicillin and streptomycin. Prior to an experiment, cells were trypsinized, centrifuged and resuspended at 1 million cells per mL. Cell passages between p8 and p12 were tested.

Device Fabrication, Operation and Data Analysis

The two-layer PDMS device (constriction channel cross-section area of 10 μm × 10 μm) was replicated from a double-layer SU-8 mold based on conventional lithography. The operation was described briefly as

follows (see Figure 1(a) and (b)). A negative pressure of 500 Pa was applied to aspirate cells continuously

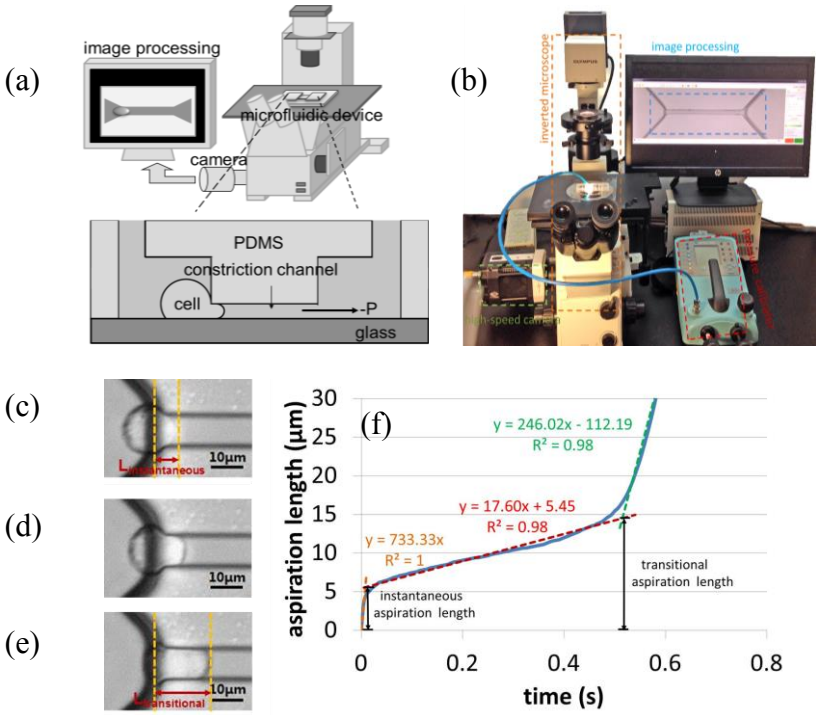

Figure 1: (a) Schematic and (b) experimental setup of the microfluidic system for continuous characterization of cellular instantaneous Young's modulus ($E_{instantaneous}$) where cells are aspirated through constriction channels with cellular entry processes monitored based on a high-speed camera. (c)-(e) Microscopic pictures of a model cell's entry process into the constriction channel, including stage I cellular initial jump into the channel (c) and stage II cellular creep increase in aspiration length (d), terminated at the transitional position (e). (f) Cellular aspiration length vs. time with $L_{instantaneous}$ and $L_{transitional}$ quantified.

through the constriction channel. Cell images were taken by an inverted microscope connected with a high-speed camera at 200 frames per sec. In order to measure cellular entry processes into the constriction channel, a background subtraction technique was developed to process the captured images including frame differencing, thresholding, particle removal using erosion, and edge detection.

Numerical Modeling

Numerical simulations were performed using ABAQUS where channels were modelled as rigid surfaces with a geometrical parameter of $D_{channel}$. The cell was modelled as an incompressible solid with a key mechanical parameter of $E_{instantaneous}$. The friction on cell-wall interface was represented by f_c.

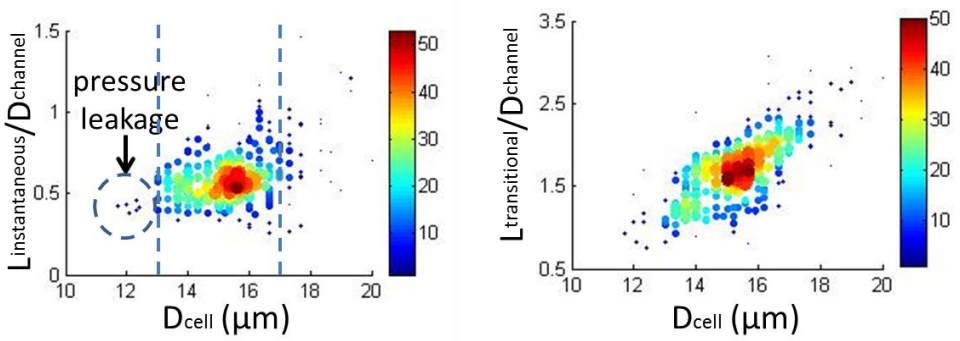

Figure 2: Scatter plots of $L_{instantaneous}/D_{channel}$ vs. D_{cell} and $L_{transitional}/D_{channel}$ vs. D_{cell} (n_{cell}=285, $D_{channel}$=10 μm) for A549 cells. For cellular diameters smaller than 13 μm, significant pressure leakage was observed while for cellular diameters larger than 17 μm, cellular breakage during the channel squeezing process was noticed. Thus, cellular diameters from 13.5 to 16.5 μm were used in future data analysis.

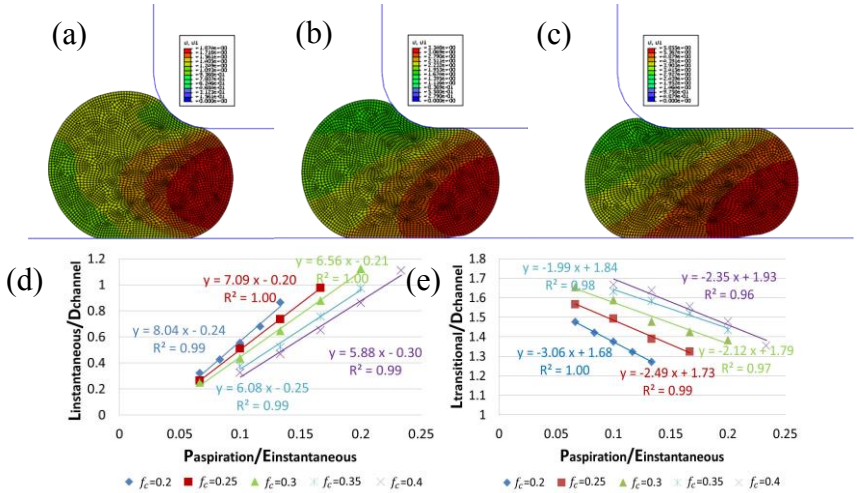

Figure 3: Numerical simulations of the cellular entry process including initial jump into the channel (a), cellular creep response (b) terminated at the transitional position (c). Numerical simulation results of $L_{instantaneous}/D_{channel}$ (d) and $L_{transitional}/D_{channel}$ (e) as functions of $P_{aspiration}/E_{instantaneous}$ (linear function) and f_c.

RESULTS AND DISCUSSION

Figure 1(c)-(e) show microscopic pictures of a representative cell's entry process into the constriction channel (A549). Based on quantified aspiration length (the distance between the cellular leading tip and the beginning of the constriction channel) vs. time (see Figure 1(f)), the entry process was divided into two stages.

In stage I, an instantaneous jump into the constriction channel was observed (see Figure 1(c)), characterized by the instantaneous aspiration length ($L_{instantaneous}$) in Figure 1(f). After the instantaneous jump, a gradual increase in aspiration length (see Figure 1(d) and (f)) was observed due to the cellular creeping behavior and was defined as stage II. With further increase in aspiration length due to cellular viscoelastic properties, a transitional position quantified as transitional aspiration length ($L_{transitional}$) was reached (see Figure 1(f)), which is the end of the creep stage and the cell started to rapidly enters the channel.

Quantified $L_{instantaneous}/D_{channel}$ and $L_{transitional}/D_{channel}$ were 0.62±0.18 and 1.72±0.43 for A549 cells (n_{cell}=285) where $D_{channel}$ represents the characteristic channel dimension (10 μm). For cellular diameters smaller than 13 μm, significantly lower values in $L_{instantaneous}/D_{channel}$ were located, indicating pressure leakage due to the improper sealing between the cellular aspiration tips with constriction channel walls. On the other hand, for cellular diameters larger than 17 μm, cellular breakage during the squeezing process due to ultra-large deformation was observed. Thus, cellular diameters ranging from 13.5 to 16.5 μm were used

in the following studies with a total cell number of 199 (see Figure 2).

Figure 3(a)-(c) show the simulation results of the cellular entry process including the stage I of instantaneous jump into the channel (Figure 3(a)) and the stage II of cellular creep response (Figure 3(b)), with the ending point at the transitional position (Figure 3(c)).

Numerical simulation results show that $P_{aspiration}/E_{instantaneous}$ and f_c affect $L_{instantaneous}/D_{channel}$ (Figure 3(d)). With an increase in $P_{aspiration}/E_{instantaneous}$, a corresponding linear increase in $L_{instantaneous}/D_{channel}$ was located with quantified coefficients as 0.99 (f_c=0.2), 1.00 (f_c=0.25), 1.00 (f_c=0.3), 0.99 (f_c=0.35) and 0.99 (f_c=0.4). Meanwhile, $L_{transitional}/D_{channel}$ was also shown to depend on $P_{aspiration}/E_{instantaneous}$ and f_c (see Figure 3(e)). With an increase in $P_{aspiration}/E_{instantaneous}$, a corresponding linear decrease in $L_{transitional}/D_{channel}$ was located with quantified coefficients as 1.00 (f_c=0.2), 0.99 (f_c=0.25), 0.97 (f_c=0.3), 0.98 (f_c=0.35) and 0.96 (f_c=0.4).

By combining measured $L_{instantaneous}$ and $L_{transitional}$ with these numerical simulation results, $E_{instantaneous}$ and f_c of A549 cells were quantified as 3.48±0.86 kPa and 0.39±0.11 for A549 cells (n_{cell}=199), 2.99±0.38 kPa and 0.37±0.02 for 95C cells (n_{cell}=164) as well as 5.24±0.74 kPa and 0.37±0.02 for 95D cells (n_{cell}=143) (see Figure 4). Statistically significant differences of $E_{instantaneous}$ for these cell types were located.

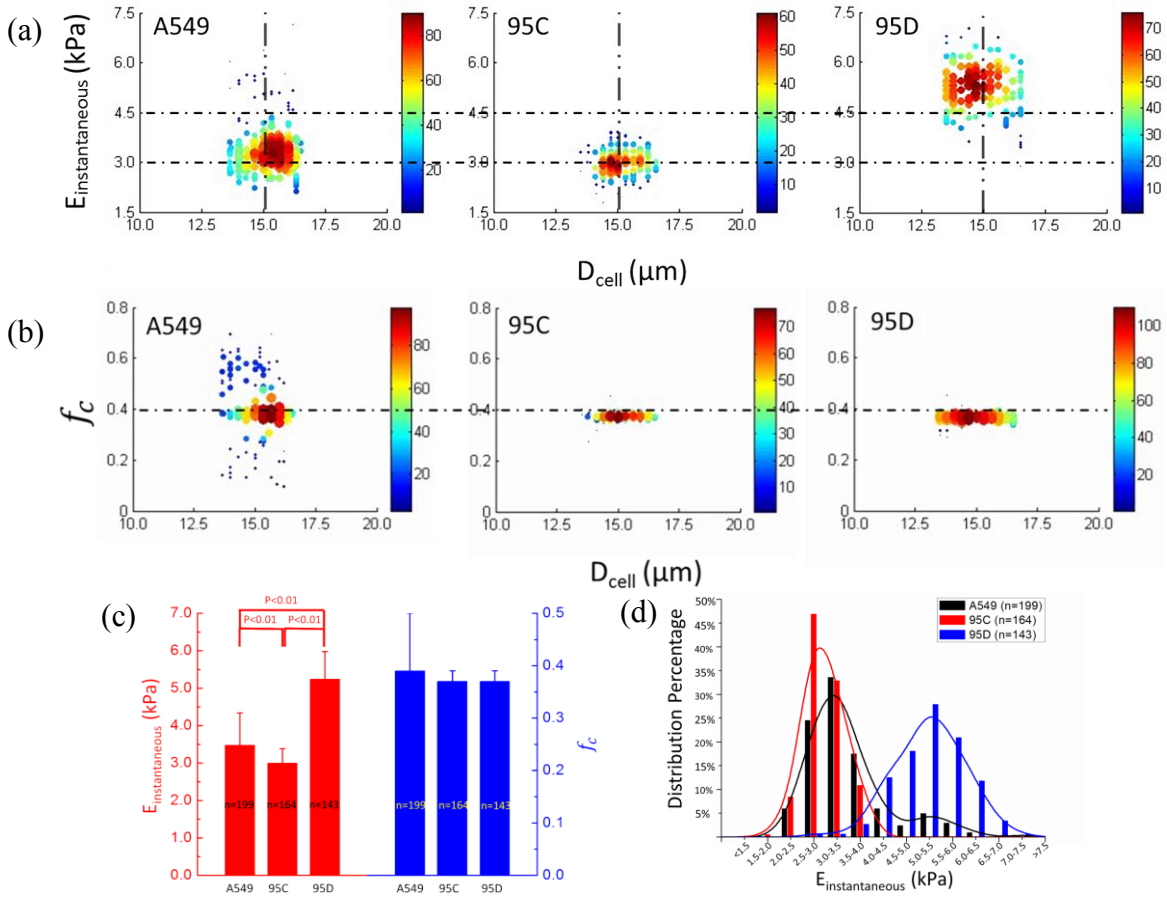

Figure 4: Scatter plots of (a) $E_{instantaneous}$ vs. D_{cell} and (b) f_c vs. D_{cell} for A549 cells (n_{cell}=199), 95C cells (n_{cell}=164) and 95D cells (n_{cell}=143). (c) and (d) Quantified $E_{instantaneous}$ with distribution for A549 cells, 95C cells and 95D cells, indicating noticeable differences in $E_{instantaneous}$ among these three cell types.

CONCLUSION

This paper demonstrated the use of the constriction channel design to quantify cellular $E_{instantaneous}$ in a continuous manner. By combining experimental results with numerical simulations, $E_{instantaneous}$ and f_c of

hundreds of tumor cells were quantified. Future work will focus on the application of this technique to quantify various cell types from a large number of single cells and explore the possibility of using cellular mechanical properties as label-free biophysical markers for cellular status evaluation and type classification.

ACKNOWLEDGMENTS

The authors would like to acknowledge financial support from National Basic Research Program of China (No. 2014CB744600) and National Natural Science Foundation of China (No. 61201077 and 81261120561).

REFERENCES

[1] S. Suresh, "Biomechanics and Biophysics of Cancer Cells", *Acta Biomaterialia*, 3, 413-438, 2007.
[2] S.E. Cross et al., "Nanomechanical Analysis of Cells from Cancer Patients", *Nature Nanotechnology*, 2, 780-783, 2007.
[3] C.T. Lim et al., "Deformability Study of Breast Cancer Cells Using Microfluidics", *Biomedical Microdevices*, 11, 557-5564, 2009.
[4] D. Di Carlo et al., "Hydrodynamic Stretching of Single Cells for Large Population Mechanical Phenotyping", *PNAS*, 109, 7630-76305, 2012.

CONTACT

* R. Long; rlong2@ualberta.ca
* J.B. WANG; jbwang@mail.ie.ac.cn
* J. CHEN; chenjian@mail.ie.ac.cn